DMD Fast Forward. Published on February 8, 2017 as DOI: 10.1124/dmd.116.074294
This article has not been copyedited and formatted. The final version may differ from this version.

Quantitative prediction of human renal clearance and drug-drug interactions of organic anion transporter substrates using *in vitro* transport data: A relative activity factor approach

Sumathy Mathialagan, Mary A Piotrowski, David A Tess, Bo Feng, John Litchfield,

Manthena V Varma

Pharmacokinetics, Pharmacodynamics, and Metabolism Department – New Chemical Entities, Pfizer Inc., Eastern Point Road, Groton, CT (SM., MP., BF., MV.) and Cambridge MA (DT., JL.)

DMD Fast Forward. Published on February 8, 2017 as DOI: 10.1124/dmd.116.074294
This article has not been copyedited and formatted. The final version may differ from this version.

Running title: Predicting renal clearance of OAT substrates

Corresponding Author: Manthena V. Varma, Pharmacokinetics, Dynamics, and Metabolism, MS 8220-2451, Pfizer Global Research and Development, Pfizer Inc., Groton, CT 06340; Phone:+1-860-715-0257. Fax: +1-860-441-6402. E-mail: manthena.v.varma@pfizer.com

Number of text pages: 17

Number of tables: 2

Number of Figures: 6

Number of references: 47

Number of words in Abstract: 210

Number of words in Introduction: 524

Number of words in Discussion: 1515

ABBREVIATIONS:

AFE, average fold error; $CL_{int,OATx}$, intrinsic active uptake clearance; $CL_{int,sec}$, intrinsic secretory clearance; $C_{max,u}$, maximum unbound plasma concentration; CL_{pass}, intrinsic passive clearance; $CL_{renal,b}$, renal blood clearance; $CL_{renal,p}$, renal plasma clearance; CL_{sec}, renal secretory clearance; DDIs, drug-drug interactions; ECCS, extended clearance classification system; $f_{u,b}$, unbound fraction in blood; F_{reabs}, fraction reabsorbed; GFR, glomerular filtration rate; HEK, human embryonic kidney; IC_{50}, inhibition constant; IVIVE, *in vitro-in vivo* extrapolation; OAT, organic anion transporter; OCT, organic cation transporter; P_{app}, apparent permeability; RAF, relative activity factor.

DMD Fast Forward. Published on February 8, 2017 as DOI: 10.1124/dmd.116.074294
This article has not been copyedited and formatted. The final version may differ from this version.

ABSTRACT

Organic anion transporters (OATs) are important in the renal secretion, and thus the clearance, of many drugs; and their functional change can result in pharmacokinetic variability. In this study, we applied transport rates measured *in vitro* using OAT-transfected human embryonic kidney cells to predict human renal secretory and total renal clearance of 31 diverse drugs. Selective substrates to OAT1 (tenofovir), OAT2 (acyclovir and ganciclovir) and OAT3 (benzylpenicillin, oseltamivir acid) were used to obtain relative activity factors (RAFs) for these individual transporters by relating *in vitro* transport clearance (after physiological scaling) to *in vivo* secretory clearance. Employing the estimated RAFs – 0.64, 7.3 and 4.1 for OAT1, OAT2 and OAT3, respectively – and the *in vitro* active clearances, renal secretory clearance and total renal clearance were predicted with an average fold error (AFE) of 1.89 and 1.40, respectively. The results show that OAT3-mediated transport play predominant role in the renal secretion for 22 of 31 drugs evaluated. This mechanistic static approach was further applied to quantitatively predict renal drug-drug interactions (AFE ~1.6) of the substrate drugs with probenecid, a clinical probe OAT inhibitor. In conclusion, the proposed static *in vitro-in vivo* extrapolation approach is the first comprehensive attempt towards mechanistic modeling of renal secretory clearance based on routinely employed *in vitro* cell models.

INTRODUCTION

Accurate prediction of human pharmacokinetic properties during the drug design stage is very important to identify and progress candidate molecules that can be successful in the clinic (Hosea et al., 2009; Di et al., 2013). With the improved understanding in metabolic biotransformation pathways, medicinal design teams are able to achieve good metabolic stability; however, such chemical space may likely possess transporter-mediated disposition as the major clearance mechanism – hepatic uptake and renal clearance (Varma et al., 2015). Kidney plays a key role in the detoxification of xenobiotics and endogenous products (Russel et al., 2002; Lee and Kim, 2004; Feng et al., 2010). In an analysis of 391 drugs with human clearance data available, ~31% (123 compounds) showed predominant renal elimination contribution (i.e., renal clearance more than 50% of total body clearance), implying the need for renal clearance projections in drug discovery (Varma et al., 2009). Renal elimination is the net result of several processes, involving glomerular filtration, active secretion and tubular reabsorption, and possibly renal metabolism (Russel et al., 2002; Lee and Kim, 2004; Feng et al., 2010; Morrissey et al., 2013).

Glomerular filtration is a unidirectional passive process that occurs for most small molecules (MW<5000 Da) regardless of their ionization state. Renal secretion is a process where transporters actively secrete compounds into the renal tubule. Solute Carrier Family 22A (SLC22A**)** transporter system, which include organic anion transporters (OATs) and organic cation transporters (OCTs), predominantly govern this process (Lee and Kim, 2004; Feng et al., 2010; Morrissey et al., 2013). Localized on the basolateral membrane of the proximal tubules, OAT1/2/3 and OCT2 are involved in the uptake of drugs, and are associated with clinical DDIs (Morrissey et al., 2013). On other hand, tubular reabsorption often depends on the passive permeability of compounds (Varma et al., 2009; Scotcher et al., 2016).

Allometric scaling using animal data is widely applied for extrapolating the pharmacokinetic parameters, including renal clearance, to predict clinical pharmacokinetics (Paine et al., 2011). Such scaling methodology may be useful for drugs that are eliminated in the urine by glomerular filtration process. However, allometry is not a reliable methodology for drug cleared predominantly by transporter-mediated active process because of possible species difference in transporter expression and function (Chu et al., 2013). Prediction of active secretion is limited by lack of established *in vitro-in vivo* extrapolation (IVIVE) methodologies. Secretion of ionic drugs involves basolateral uptake and subsequent efflux across the apical membrane into the urine. However, the renal uptake clearance of anionic drugs is typically similar to renal secretory clearance with uptake often being the rate-determining process (Sirianni and Pang, 1997; Watanabe et al., 2011; Varma et al., 2015). Therefore, establishing IVIVE of basolateral uptake clearance alone could provide quantitative prediction of renal secretory clearance.

Our goal is to establish an *IVIVE* method based on relative activity factor (RAF) to predict human renal clearance of OAT substrates using *in vitro* transport data. Transporter-specific uptake clearance was measured in human embryonic kidney (HEK)293 cells singly transfected with human OAT1, OAT2 and OAT3, and scaled to *in vivo* secretory clearance via RAFs – established using selective substrates. This bottom-up approach was further extended to predict OAT-mediated drug interactions with probenecid, a recommended probe inhibitor.

DMD Fast Forward. Published on February 8, 2017 as DOI: 10.1124/dmd.116.074294
This article has not been copyedited and formatted. The final version may differ from this version.

MATERIALS AND METHODS

Materials

HEK293 cells transfected with OAT1 and OAT3 were obtained from Dr. Kathleen Giacomini (UCSF, CA). HEK293 cells transfected with OAT2-variant 1 were obtained from Dr. Ryan Pelis (Halifex, Canada). All the compounds used in the assay were obtained from Pfizer chemical inventory system or procured from Sigma-Aldrich (St.Louis, MO). Biocoat poly-D-lysine 48-well plates were obtained from Corning Inc (Corning, NY). Fetal bovine serum was purchased from Sigma-Aldrich (St.Louis, MO). DMEM (Dulbecco's Modified Eagle Medium), Hygromycin B, Gentamicin and sodium pyruvate were obtained from Gibco life technologies (Waltham, MA). HBSS (Hank's Balanced Salt Solution), HEPES, 4-(2-Hydroxyethyl)piperazine-1-ethanesulfonic acid) were obtained from Lonza Inc. (Allendale, NJ). ^{3}H-Para aminohippuric acid, ^{3}H-Estrone sulfate and ^{3}H-cGMP were purchased from Perkin-Elmer Inc. (Waltham, MA).

Clinical data collection

Human renal clearance and the plasma fraction unbound of the drugs were primarily taken from our previous compilations (Obach et al., 2008; Varma et al., 2009; Lombardo et al., 2014) and additional literature publications. Where available, human blood-to-plasma (BP) ratio was extracted from literature or from internal database. BP ratio was assumed to be 0.55 for anionic drugs and 1 for non-acidic drugs when the experimental data was not available. However, no significant impact of BP ratio was noted on the overall predictions. DDI (percentage change in renal clearance) data was collected primarily from University of Washington drug interaction database (https://www.druginteractioninfo.org) and additional Pubmed search.

Transport studies using OATs transfected HEK293 cells

Large batches of cryopreserved OATs-transfected and wild-type HEK293 cells were prepared and validated for their transport activity before and after batch preparation. All the uptake studies were carried out using the same batch of cells per cell type according to the procedures reported earlier (Feng et al., 2008; Cheng et al., 2012). Cryopreserved HEK293 cells were directly seeded in 48-well poly-D-lysine-coated plates 48 h before each experiment, at densities of 1.2×10^5 cells/well in a volume of 0.2 mL/well. Cell monolayer confluence was verified visually under the microscope. Transport buffer was prepared at pH 7.4 using HBSS supplemented with 20 mM HEPES, and 5.55 mM dextrose. All experiments were carried out at 1 or 3 μM substrate concentration, which is typically below the reported Km values of some known OATs substrates. Immediately before the experiment, the cells were washed twice with 1 mL Dulbecco's phosphate-buffer saline (DPBS) buffer and then incubated with 100 μL DPBS buffer containing test compound at 37°C. At different time points, the cellular uptake was terminated by washing the cells three times with 0.2 mL each of ice-cold DPBS and lysed directly on the plate with 100% methanol containing internal standard and samples were quantified by LC-MS/MS methodology. For each compound, cellular uptake was measured at 6 different time point in duplicates per cell-type. Controls (3H-Para aminohippuric acid (2 μM), 3H-cGMP (2 μM) or 3H-Estrone sulfate (0.2 μM) for OAT1, OAT2 and OAT3, respectively) were run in each study to assess the assay variability and qualify the utility of rate data for secretory clearance predictions. No correction was applied, while the controls yielded rates within 30% of the mean across different days (data not shown).

LC-MS/MS analysis was conducted using a Sciex 5500 triple quadrupole tandem mass spectrometer in electrospray ionization (ESI) mode. Other instrumentation consisted of Shimadzu LC-20AD pumps and ADDA autosampler. Liquid chromatography was performed either using a Phenomenex Kinetex C18 or a Synergi Polar (30x2mm) analytical column. Analytes were eluted with a gradient profile starting with 0.1% formic acid in water and increasing concentration of 0.1% formic acid in acetonitrile.

Inhibition studies using OATs transfected HEK293 cells

Inhibition studies were carried out in poly-D-lysine coated 96-well plates with HEK293 cells seeded at densities of 0.60 x10^5 cells/well, in a volume of 0.1 mL/well. The required final assay concentrations of probenecid were prepared using transport buffer spiked with probe substrates, ^{3}H-Para aminohippuric acid (2 μM), ^{3}H-cGMP (2 μM) or ^{3}H-Estrone sulfate (0.2 μM) in OAT1, OAT2 and OAT3 cells, respectively. All solutions contained a final concentration of DMSO below 1% (v/v). Uptake was started by the addition of 0.1 mL probe-spiked transport buffer without or with probenecid. The plates were then incubated for 4 min at 37ºC with shaking at 150 rpm. The experiment was stopped by the removal of transport buffer followed by three washes with 0.15 mL/well ice-cold uptake buffer. Samples were retrieved by lysing the cells with 0.1 mL of 10 mM Tris-HCL pH 7.5, 75 mM NaCl, 125 mM NaF, 2.5 mM EDTA, and 0.5% tergitol-type NP40. Radioactivity in each sample was quantified by measurement on a Perkin Elmer MicroBeta TriLux Liquid Scintillation Counter.

Mechanistic model to estimate *in vitro* transport clearances

DMD Fast Forward. Published on February 8, 2017 as DOI: 10.1124/dmd.116.074294
This article has not been copyedited and formatted. The final version may differ from this version.

A 2-compartment model (compartments representing the media and cell) was developed to estimate the intrinsic passive clearance (CL_{pass}) and intrinsic active uptake clearance via individual transporters ($CL_{int,OAT1}$, $CL_{int,OAT2}$, $CL_{int,OAT3}$), by simultaneously fitting the cell accumulation data (A_{cell}) from all 4 cell lines. This model is analogous to the method described previously to analyze transport data in other cell systems (Poirier et al., 2008). Equations 1-6 are used in this modeling process:

$$V_{ew} \cdot \frac{dC_{ew}}{dt} = -\left(CL_{pass} + CL_{int,OAT}\right) \cdot C_{ew} \cdot f_{u,ew} + CL_{pass} \cdot C_{iw} \cdot f_{u,c} \quad \text{(Eq. 1)}$$

$$V_{iw} \cdot \frac{dC_{iw}}{dt} = \left(CL_{pass} + CL_{int,OAT}\right) \cdot C_{ew} \cdot f_{u,ew} - CL_{pass} \cdot C_{iw} \cdot f_{u,c} \quad \text{(Eq. 2)}$$

$$f_{u,ew} = \frac{1}{\left(1+K_{a,mem} \cdot PR/V_{ew}+K_{a,trans} \cdot PR/V_{ew}\right)} \quad \text{(Eq. 3)}$$

$$V_{iw} = PR \cdot CpPR \cdot VpC \quad \text{(Eq. 4)}$$

$$A_{cell} = A_{iw} + A_{ew} \cdot \left(1 - f_{u,ew}\right) \quad \text{(Eq. 5)}$$

$$\text{and, } C_{ew} = \frac{A_{ew}}{V_{ew}};\ C_{iw} = \frac{A_{iw}}{V_{iw}} \quad \text{(Eq. 6)}$$

Where, C_{ew}, C_{iw}, A_{ew}, A_{iw}, V_{ew} (0.2 mL) and V_{iw} repesent concentration, amount and volume of the extracellular and intracellular compartments. $f_{u,ew}$ and $f_{u,c}$ are extracellular and intracellular unbound fractions. $K_{a,mem}$ represent non-specific binding affinity to cell membranes and $K_{a,trans}$ is non-specific binding affinity to transfected transporter. *PR* is the measured protein concentration per well. *CpPR* is cells per measured protein (4 million cells/mg) and *VpC* is cell volume (1.7µL/million cells) measured assuming sperical stucture (14.8µm diameter).

Prediction of renal clearance and drug interactions

DMD Fast Forward. Published on February 8, 2017 as DOI: 10.1124/dmd.116.074294
This article has not been copyedited and formatted. The final version may differ from this version.

Renal blood clearance ($CL_{renal,b}$) is determined by glomerular filtration, tubular secretion, and reabsorption processes, and can be mathematically described by (Russel et al., 2002; Feng et al., 2010):

$$\mathrm{CL_{renal,b}} = (\mathrm{f_{u,b}}.\mathrm{GFR} + \mathrm{CL_{sec}}) \cdot (1 - \mathrm{F_{reabs}}) \quad \text{(Eq. 7)}$$

Where, $f_{u,b}$ is unbound fraction in blood, *GFR* is glomerular filtration rate, CL_{sec} is renal secretory clearance and F_{reabs} is the fraction of filtered and secreted drug that is reabsorbed. $CL_{renal,b}$ is equal to renal plasma clearance ($CL_{renal,p}$) divided by blood-to-plasma ratio. For the majority of compounds tested in this study, passive permeability or passive transport clearance is very low and so the F_{reabs} was assumed to be negligible (see Results and Discussion). Assuming a well-stirred model, CL_{sec} is expressed as (Eq. 8):

$$\mathrm{CL_{sec}} = \mathrm{Q_r} \cdot \frac{\mathrm{f_{u,b}} \cdot \mathrm{CL_{int,sec}}}{\mathrm{Q_r} + \mathrm{f_{u,b}} \cdot \mathrm{CL_{int,sec}}} \quad \text{(Eq. 8)}$$

Where Q_r is the renal blood flow (15.7 mL/min/kg (Davies and Morris, 1993)) and $CL_{int,sec}$ is the intrinsic secretory clearance obtained from *in vitro* uptake studies. *In vitro* active uptake clearance (µL/min/mg-protein) mediated by each OAT was corrected using physiological scalars to obtain *in vitro* scaled $CL_{int,OATx}$ in the units of mL/min/kg: 0.25 mg-protein per million HEK293 cells (measured), 1 million HEK293 cells per million proximal tubule cells (assumed), 60 million proximal tubule cells per gram kidney and 4.3 gram kidney per kilogram body weight (Davies and Morris, 1993; Imamura et al., 2011; Watanabe et al., 2011). *In vitro* $CL_{int,sec}$ was estimated from the *in vitro* active uptake clearance of individual OATs and the relative activity factors (RAF) of the corresponding transporter.

$$\mathrm{CL_{int,sec}} = \mathrm{CL_{int,OAT1}}.\mathrm{RAF_{OAT1}} + \mathrm{CL_{int,OAT2}}.\mathrm{RAF_{OAT2}} + \mathrm{CL_{int,OAT3}}.\mathrm{RAF_{OAT3}} \quad \text{(Eq. 9)}$$

RAF for a given OAT was estimated from the *in vivo* $CL_{int,sec}$ and the *in vitro* uptake clearance of one or multiple selective substrate(s) for that transporter, as follows.

$$\mathrm{RAF_{OATx}} = \frac{\text{In vivo}\,\mathrm{CL_{int,sec}}}{\text{In vitro}\,\mathrm{CL_{int,OATx}}} \qquad \text{(Eq. 10)}$$

Prediction of change in renal clearance in the presence of probenecid, a recommended probe inhibitor for OATs-based interactions, was calculated using the following set of equations.

$$\mathrm{CL'_{int,sec}} = \frac{\mathrm{CL_{int,OAT1}}.\mathrm{RAF_{OAT1}}}{\left(1+\frac{\mathrm{C_{max,u}}}{\mathrm{IC_{50}}}\right)} + \frac{\mathrm{CL_{int,OAT2}}.\mathrm{RAF_{OAT2}}}{\left(1+\frac{\mathrm{C_{max,u}}}{\mathrm{IC_{50}}}\right)} + \frac{\mathrm{CL_{int,OAT3}}.\mathrm{RAF_{OAT3}}}{\left(1+\frac{\mathrm{C_{max,u}}}{\mathrm{IC_{50}}}\right)} \qquad \text{(Eq. 11)}$$

$$\mathrm{CL'_{sec}} = \mathrm{Q_r}\cdot\frac{\mathrm{f_{u,b}}\cdot\mathrm{CL'_{int,sec}}}{\mathrm{Q_r}+\mathrm{f_{u,b}}\cdot\mathrm{CL'_{int,sec}}} \qquad \text{(Eq. 12)}$$

$$\%\ \text{change in renal clearance} = \frac{\left(\mathrm{CL_{sec}}+\mathrm{f_{u,b}}.\mathrm{GFR}\right)-\left(\mathrm{CL'_{sec}}+\mathrm{f_{u,b}}.\mathrm{GFR}\right)}{\left(\mathrm{CL_{sec}}+\mathrm{f_{u,b}}.\mathrm{GFR}\right)} \qquad \text{(Eq. 13)}$$

CL'$_{int,sec}$ and *CL'$_{sec}$* are intrinsic secretory and overall secretory clearance in the presence of the inhibitor drug, respectively. IC_{50} is the inhibition constant and $C_{max,u}$ is the maximum unbound plasma concentration of inhibitor drug.

Model Predictability

Prediction bias and precision were assessed with average fold error (AFE) Eq. 14.

$$\mathrm{AFE} = 10^{\frac{1}{\mathrm{N}}\Sigma\left|\mathrm{Log_{10}}\frac{\mathrm{Predicted}}{\mathrm{Observed}}\right|} \qquad \text{(Eq. 14)}$$

N is the number of observations.

DMD Fast Forward. Published on February 8, 2017 as DOI: 10.1124/dmd.116.074294
This article has not been copyedited and formatted. The final version may differ from this version.

RESULTS

In vitro transport of OAT substrates

Uptake of 31 drugs was evaluated in wild-type and transporter-transfected HEK293 cell expressing OAT1, OAT2 and OAT3. Tenofovir showed selective uptake by OAT1-transfectd cells, while its uptake by OAT2- and OAT3-transfected cells was not significantly (*F*-test with α-value of 0.05) different from the uptake by wild-type cells. Similarly, acyclovir and ganciclovir showed selective uptake by OAT2. Benzylpenicillin (penicillin G) and oseltamivir acid were selectively transported by OAT3 (Fig. 1). Data were fitted to a two-compartment model to estimate the transporter-mediated active uptake clearance ($CL_{int,OAT}$) and passive uptake clearance (CL_{pass}). Table 1. shows the estimated uptake clearance of the 5 selective substrates as well as other 26 compounds evaluated in this study. The *in vitro* active uptake clearance was scaled to obtain the *in vivo* value per body weight using the physiological scaling factors. Using the selective substrates, relative activity factors (RAFs) were derived to bridge the difference between the scaled *in vitro* uptake clearance and the *in vivo* intrinsic secretory clearance for each transporter. The obtained RAFs are 0.64, 7.3 and 4.1 for OAT1, OAT2 and OAT3, respectively.

Prediction of active secretion and renal clearance

Secretory intrinsic clearance ($CL_{int,sec}$) and the renal plasma clearance predicted using the transport data and the obtained RAFs showed good agreement to the observed values (Fig. 2). The predicted $CL_{int,sec}$ and renal clearance are within 2-fold for 68% and 84% of the observed values, respectively, for the 31 compounds evaluated. Acetazolamide, adefovir, bumetanide, pravastatin, rosuvastatin and zalcitabine are notable outliers, while the predicted intrinsic secretory clearance for other 25 compounds were within 3-fold of the observed

DMD Fast Forward. Published on February 8, 2017 as DOI: 10.1124/dmd.116.074294
This article has not been copyedited and formatted. The final version may differ from this version.

values (Fig 2A). Acetazolamide is the only compound showing >3-fold underprediction of renal clearance (Fig. 2B).

Fig. 3. depicts the predicted percentage contribution of the individual OATs and glomerular filtration to the human renal clearance. Interestingly, none of the compounds tested exhibited measurable contribution of all three OATs for their renal clearance. Finally, OAT3-mediated transport emerged as the predominant driver to active secretion of 22 compounds.

Permeability – tubular reabsorption relationship

Using a separate dataset of 47 compounds with human renal plasma clearance lower than $f_{u,p} \cdot GFR$ (Supplementary Table 1), an empirical relationship between fraction reabsorbed [F_{reabs} = 1-($CL_{renal,p}$/ $f_{u,p}.GFR$)] and apparent permeability (P_{app}) across MDCK-low efflux cells (pH 6.5) was derived. Permeability values were obtained from our previous work (Varma et al., 2012). We applied sigmoidal model [$F_{reabs} = {P_{app}}^{a}/({b^a} + {P_{app}}^{a})$, where '*a*' represents the slope factor and '*b*' is the value of P_{app} at which F_{reabs} equals 0.5] that was previously reported (Scotcher et al., 2016). Similar to the finding of Scotcher et al. (Scotcher et al., 2016), no correlation was seen for basic drugs. However, a significant correlation (r^2=0.9) was noted for the combined set of acids, neutral and zwitterions (n=31), with the estimated values of 2.9 ± 0.6 and 6.0 ± 0.5 x10^{-6} cm/sec for '*a*' and '*b*', respectively (Fig. 4A). On the basis of this relationship, we note that the tubular reabsorption of majority of compounds (28 of 31) in the OATs (renal secretory) dataset is <0.15 (Fig. 4B).

Prediction of renal DDIs with probenecid

In vitro inhibition studies showed concentration-dependent inhibition of OAT1-mediated PAH uptake and OAT3-mediated E3S uptake by probenecid with the estimated IC_{50} values of 9.6 μM and 4.5 μM, respectively (Fig. 5). Probenecid also inhibited OAT2-

mediated cGMP uptake in the HEK293 cells, however, with a low inhibition potency (IC_{50} ~853 μM). Change in renal clearance when co-administered with probenecid was estimated using these IC_{50} values for each OAT isoform and the clinically observed free C_{max} for the corresponding dose of probenecid. Free drug hypothesis was assumed, and the DDI predictions are based on clinically observed free maximum plasma concentration of probenecid. Free C_{max} was estimated based on the observed pharmacokinetics at different doses of probenecid (Selen et al., 1982) adjusted for concentration-dependent plasma unbound fraction (Emanuelsson et al., 1987). Hence, free C_{max} values of 6.2 μM, 15 μM, 24.4 μM and 51 μM were used for the corresponding perpetrator (probenecid) dose of 500 mg, 750 mg, 1000 mg and 1500 mg, respectively. Clinical data of change in renal clearance when dosed in combination with probenecid were extracted from the published literature, for the OATs substrates evaluated in the *in vitro* rate study. A total of 18 clinical interactions with probenecid as an inhibitor drug were evaluated with the mechanistic DDI model (Eq. 11-13), which captured the filtration and secretory components of the victim drug and interaction at the level of three OAT isoforms. Predicted change in renal clearance was within ±40% of the observed mean value for 16 of 18 (89%) cases, with an AFE of 1.66, when using this mechanistic static model (Fig. 6). Acyclovir, which is predominantly transported by OAT2, is the only false negative prediction (predicted <25% and observed ≥25%).

DISCUSSION

Renal clearance determines the pharmacokinetics of several drugs, particularly Extended clearance classification system (ECCS) class 3A, 3B and 4 drugs (Varma et al., 2009; Varma et al., 2015). However, methodologies to predict renal clearance are limited with allometirc scaling of dog or rat renal clearance suggested to be a potential option (Paine et al., 2011). Our goal is to establish an IVIVE methodology to quantitatively predict renal clearance for drugs undergoing active secretion, primarily driven by OATs-mediated transport. In this process, we (i) obtained transport rates employing HEK293 cells stably transfected with individual human OATs, (ii) identified selective substrates for each of the three OATs expressed on the basolateral membrane of proximal tubule cells, and (iii) established RAFs for the three OATs using the *in vitro* active transport and *in vivo* secretory clearance of the selective substrates. The obtained RAFs and the *in vitro* transport data were then used to predict renal clearance and assess the contribution of individual OATs to the secretion for 31 drugs. Finally, this approach was extended to predict renal DDIs between these substrate drugs and probenecid – a recommended clinical OATs probe inhibitor.

Of the drugs evaluated in OAT1, OAT2 and OAT3 substrate assays, tenofovir was identified as selective substrate to OAT1, while acyclovir and ganciclovir behaved as OAT2 selective substrates. Benzyl penicillin and oseltamivir acid were selective to OAT3, with no measurable active uptake in the OAT1- and OAT2-transfected cells (Fig. 1). These observations are generally consistent with the earlier reports (Cheng et al., 2012; Maeda et al., 2014). RAFs – bridging the *in vitro* and *in vivo* human intrinsic secretory clearance after correcting for the physiological scalars – were obtained using these selective substrates. The RAF values represent a collated correction for the (i) differences in the transporter expression levels between the *in vitro* transfected cells and proximal tubule cells, (ii) *in vitro-in vivo*

differences in transport activity per protein expressed, and (iii) uncertainty in the physiological parameters (eg. cells per gram kidney) needed for scaling *in vitro* data. The prediction accuracy in the active secretion clearance and the total renal clearance in terms of AFE is 1.89 and 1.41, respectively.

Early predictions of renal clearance is important for optimizing the total body clearance in a chemical series and facilitate dose projections, as well as, evaluating DDI risk. ECCS framework suggests that drugs with low passive permeability are likely cleared by urinary route (>70% of the systemic clearance), with the exception of high molecular weight (>400Da) acids or zwitterions (Class 3B); in which case, hepatic uptake may be the rate-determining process to the systemic clearance (Varma et al., 2015). Therefore, ECCS provides an early indication of the potential contribution of the renal clearance to the total body clearance and the renal DDI liability, which needs to be followed up with quantitative predictions. Availability of IVIVE methodologies for quantitative predictions is very limited. Watanabe et al., applied IVIVE approach based on *in vitro* uptake clearance by human kidney slices to predict secretory renal clearance for a set of 10 anionic drugs and showed good predictability (Watanabe et al., 2011). However, such methodology is limited by availability of human kidney tissue. Kunze et al., used *in vitro* bidirectional permeability across LLC-PK1 cells to establish a model incorporating both active secretion and tubular reabsorption to predict renal clearance of about 20 drugs (Kunze et al., 2014). Although simple and amenable to high throughput screening platforms, the later methodology, which assumes that LLC-PK1 cells (derived from pig kidney epithelium) quantitatively express all relevant uptake and efflux transporters as in human proximal tubule cells, may potentially mispredict active secretion. For example, LLC-PK1 cells show limited OAT activity and may underestimate active transport for acids and zwitterions (Hori et al., 1993). Additionally, differential expression of apical ABC and SLC transporters influence the transcellular permeability *in*

DMD Fast Forward. Published on February 8, 2017 as DOI: 10.1124/dmd.116.074294
This article has not been copyedited and formatted. The final version may differ from this version.

vitro, although uptake into cell compartment is often the rate-determining step in the secretory clearance (Watanabe et al., 2011; Posada et al., 2015). Use of established scaling factors for predicting *in vivo* clearance from the recombinant systems is a well proven practice for metabolic pathways (Obach et al., 1997). However, such IVIVE approaches are very limited for transporter-mediated clearance. Posada et al., applied initial rate data obtained from OAT3-transfected cells to develop a middle-out PBPK model to recover renal clearance of a single substrate drug, pemetrexed (Posada et al., 2015). To the best knowledge, the current study represents the first comprehensive attempt to establish IVIVE methodology for prospective translation of transport data based on stably transfected cell systems to quantitatively predict transporter-mediated renal clearance and DDIs.

The proposed IVIVE approach relies on certain assumptions, which needs careful consideration on its application. Primarily, the renal clearance of the drugs assessed here was assumed to be driven by glomerular filtration and tubular secretion process with no tubular reabsorption. It is generally believed that reabsorption is associated largely with passive transport along the length of nephron. We therefore, used an apparent relationship between transcellular permeability and fraction reabsorbed ($P_{app} - F_{reabs}$ correlation) (Scotcher et al., 2016), to demonstrate that tubular reabsorption has a minimal role in the renal clearance of drugs in our dataset (Fig. 4). A separate dataset of compounds with renal clearance lower than glomerular filtration (i.e. net reabsorption) was developed, and $P_{app} - F_{reabs}$ correlation was established using transcellular permeability measured in low efflux MDCK cells (Varma et al., 2012). Based on this relationship, we note that most of the compounds in the OATs IVIVE dataset are predicted to have F_{reabs} of less than 0.15 (Fig 4B), and thus reabsorption was not considered in the overall renal clearance predictions. However, static or dynamic reabsorption models may be applied in conjunction to the active secretion translation to predict renal clearance of compounds with high permeability (Scotcher et al., 2016). It should

be emphasized that renal clearance contribution to the total body clearance is generally <30% for moderate and high permeable drugs (P_{app} >5x10^{-6} cm/sec), as defined by BDDCS and ECCS (Wu and Benet, 2005; Varma et al., 2012; Varma et al., 2015); and therefore, need for early prediction of renal clearance in this space is generally less. Secondly, we assumed that unidirectional transport across basolateral membrane of proximal tubule cells, but not apical membrane, is the rate-determining step for the secretory clearance (i.e. loss from the blood compartment). Although some of the evaluated compounds are known substrates to efflux transporters on the apical membrane of proximal tubule cells (Supplementary Table 2), this assumption is generally accepted, particularly for OAT substrates (Sirianni and Pang, 1997; Watanabe et al., 2011; Varma et al., 2015). Finally, it was also assumed that the tubular secretion is determined by OATs-mediated transporter only, while other SLCs on the basolateral membrane of proximal tubule has minimal role. Based on the available literature and our internal data these drugs are not substrates to the other clinically relevant transporter (OCT2), with the exception of cimetidine and famotidine (Supplementary Table 2). Nevertheless, RAF for OCT2 can also be established adopting the approach described here for OATs. Other basolateral transporters, such as OATP4C1, may also contribute to the renal secretion of certain drugs (Mikkaichi et al., 2004); however, limited data is available on the OATP4C1 transport activity for the 31 compounds evaluated here. Yet challenging, quantitative understanding of the contribution of other basolateral uptake transporters and apical efflux and reabsorption transport on the clearance from the blood compartment may further improve the predictions.

Recent reports suggest role of OAT2 in the renal secretion of creatinine (Lepist et al., 2014) and some antiviral drugs (Cheng et al., 2012). We assessed the contribution of OAT2 to renal clearance of the compounds in our dataset (Fig. 3). Interestingly, only acyclovir, ganciclovir, penciclovir and ketorolac showed significant OAT2-mediated transport, with

OAT2 contributing almost entirely to the active secretion for all, except ketorolac. Similarly, only five compounds showed significant contribution of OAT1 (i.e. adefovir, cilostazol, ketoprofen, tenofovir and ketorolac). Interestingly, no single compound had notable contribution from all three transporters. ECCS class 1A and 3A compounds (low molecular weight acids/zwitterions) show major involvement of OAT1 or OAT3, while class 4 compounds (low permeable bases/neutrals) are secreted by either OAT2 or OAT3. However, all class 3B compounds (high molecular weight, low permeable acids/zwitterions) are predominantly secreted by OAT3 alone. Overall, OAT3 emerged as a major contributor for the renal secretion for majority of the compounds evaluated, implying its clinical significance for wide variety of drugs.

Regulatory guidelines suggest *in vitro* and follow up clinical assessment for the OAT1 and OAT3 mediated clearance of investigational drugs (EMA, 2012; USFDA, 2012). Probenecid can potently inhibit OAT1 and OAT3 *in vivo* and can serve as a clinical probe inhibitor for these two transporters. The *in vivo* inhibition potency ($1+C_{max,u}/IC_{50}$) of probenecid (1.5 g dose) can reach up to about 6 and 12 fold against OAT1 and OAT3, respectively, implying that an estimated ~84% (OAT1) and >90% (OAT3) of the transporter-mediated secretory clearance can be inhibited by probenecid at a clinically relevant dose. On the other hand, probenecid only had a minimal inhibition of OAT2-mediated renal secretion (<5% inhibition). Therefore, alternative clinical probe inhibitor should be considered when the investigational drug is selectively or predominantly transported by OAT2 (eg. acyclovir, ganciclovir). A review of literature suggested indomethacin as the only plausible clinical probe inhibitor. However, based on the *in vitro* IC_{50} (2.1 μM) (Shen et al., 2015) and free C_{max} (0.7 μM), it may only cause ~30% inhibition of OAT2 at its therapeutic dose.

In conclusion, to our best knowledge this is the first report providing a comprehensively validated IVIVE method that allows for quantitative prediction of human

DMD Fast Forward. Published on February 8, 2017 as DOI: 10.1124/dmd.116.074294
This article has not been copyedited and formatted. The final version may differ from this version.

renal clearance and DDIs, on the basis of *in vitro* transport data obtained using transporter-transfected cell systems. Additionally, this static mechanistic approach provides a basis for dynamic physiological-based modeling of renal secretory clearance and DDIs.

ACKNOWLEDGMENTS

Authors would like to thank David Rodrigues, Larry Tremaine and Tristan Maurer for valuable inputs during this work.

AUTHORSHIP CONTRIBUTIONS

Participated in research design: Mathialagan, Tess, Litchfield, and Varma.

Conducted experiments: Mathialagan, Piotrowski.

Contributed new reagents or analytic tools: Mathialagan, Tess, and Varma.

Performed data analysis: Mathialagan, Feng, and Varma.

Wrote or contributed to the writing of the manuscript: Mathialagan, Piotrowski, Tess, Feng, Litchfield, and Varma.

REFERENCES

Aherne GW, Piall E, Marks V, Mould G and White WF (1978) Prolongation and enhancement of serum methotrexate concentrations by probenecid. *Br Med J* **1**:1097-1099.

Brown G, Zemcov SJ and Clarke AM (1993) Effect of probenecid on cefazolin serum concentrations. *J Antimicrob Chemother* **31**:1009-1011.

Cheng Y, Vapurcuyan A, Shahidullah M, Aleksunes LM and Pelis RM (2012) Expression of organic anion transporter 2 in the human kidney and its potential role in the tubular secretion of guanine-containing antiviral drugs. *Drug Metab Dispos* **40**:617-624.

Chennavasin P, Seiwell R, Brater DC and Liang WM (1979) Pharmacodynamic analysis of the furosemide-probenecid interaction in man. *Kidney Int* **16**:187-195.

Chu X, Bleasby K and Evers R (2013) Species differences in drug transporters and implications for translating preclinical findings to humans. *Exp Opin Drug Met Tox* **9**:237-252.

Cimoch PJ, Lavelle J, Pollard R, Griffy KG, Wong R, Tarnowski TL, Casserella S and Jung D (1998) Pharmacokinetics of oral ganciclovir alone and in combination with zidovudine, didanosine, and probenecid in HIV-infected subjects. *J Acquir Immune Defic Syndr Hum Retrovirol* **17**:227-234.

Davies B and Morris T (1993) Physiological parameters in laboratory animals and humans. *Pharm Res* **10**:1093-1095.

Di L, Feng B, Goosen TC, Lai Y, Steyn SJ, Varma MV and Obach RS (2013) A perspective on the prediction of drug pharmacokinetics and disposition in drug research and development. *Drug Metab Dispos* **41**:1975-1993.

EMA (2012) Guideline on the investigation of drug interactions. *http://wwwemaeuropaeu/docs/en_GB/document_library/Scientific_guideline/2012/07/WC500129606pdf Committee for Human Medicinal Products (CHMP), London, UK*.

Emanuelsson BM, Beermann B and Paalzow LK (1987) Non-linear elimination and protein binding of probenecid. *Eur J Clin Pharmacol* **32**:395-401.

Feng B, LaPerle JL, Chang G and Varma MV (2010) Renal clearance in drug discovery and development: molecular descriptors, drug transporters and disease state. *Exp Opin Drug Met Tox* **6**:939-952.

Feng B, Obach RS, Burstein AH, Clark DJ, de Morais SM and Faessel HM (2008) Effect of Human Renal Cationic Transporter Inhibition on the Pharmacokinetics of Varenicline, a New Therapy for Smoking Cessation: An In Vitro-In Vivo Study. *Clin Pharmacol Ther* **83**:567-576.

Gisclon LG, Boyd RA, Williams RL and Giacomini KM (1989) The effect of probenecid on the renal elimination of cimetidine. *Clin Pharmacol Ther* **45**:444-452.

Hill G, Cihlar T, Oo C, Ho ES, Prior K, Wiltshire H, Barrett J, Liu B and Ward P (2002) The anti-influenza drug oseltamivir exhibits low potential to induce pharmacokinetic drug interactions via renal secretion-correlation of in vivo and in vitro studies. *Drug Metab Dispos* **30**:13-19.

Hori R, Okamura M, Takayama A, Hirozane K and Takano M (1993) Transport of organic anion in the OK kidney epithelial cell line. *Am J Physiol-Renal Physiol* **264**:F975-F980.

Hosea NA, Collard WT, Cole S, Maurer TS, Fang RX, Jones H, Kakar SM, Nakai Y, Smith BJ, Webster R and Beaumont K (2009) Prediction of human pharmacokinetics from preclinical information: comparative accuracy of quantitative prediction approaches. *J Clin Pharmacol* **49**:513-533.

Imamura Y, Murayama N, Okudaira N, Kurihara A, Okazaki O, Izumi T, Inoue K, Yuasa H, Kusuhara H and Sugiyama Y (2011) Prediction of Fluoroquinolone-Induced Elevation in Serum Creatinine Levels: A Case of Drug–Endogenous Substance Interaction Involving the Inhibition of Renal Secretion. *Clinical Pharmacology & Therapeutics* **89**:81-88.

Inotsume N, Nishimura M, Nakano M, Fujiyama S and Sato T (1990) The inhibitory effect of probenecid on renal excretion of famotidine in young, healthy volunteers. *J Clin Pharmacol* **30**:50-56.

Kunze A, Huwyler J, Poller B, Gutmann H and Camenisch G (2014) In vitro–in vivo extrapolation method to predict human renal clearance of drugs. *J Pharm Sci* **103**:994-1001.

Laskin OL, de Miranda P, King DH, Page DA, Longstreth JA, Rocco L and Lietman PS (1982) Effects of probenecid on the pharmacokinetics and elimination of acyclovir in humans. *Antimicrob Agents Chemother* **21**:804-807.

Lee W and Kim RB (2004) Transporters and renal drug elimination. *Annu Rev Pharmacol Toxicol* **44**:137-166.

Lepist E-I, Zhang X, Hao J, Huang J, Kosaka A, Birkus G, Murray BP, Bannister R, Cihlar T and Huang Y (2014) Contribution of the organic anion transporter OAT2 to the renal active tubular secretion of creatinine and mechanism for serum creatinine elevations caused by cobicistat. *Kidney int* **86**:350-357.

Li KY, Qiu Y, Jiang Y, Luo CH, Lin XP, Wang J and Yang N (2014) Effect of probenecid on pharmacokinetics and tolerability of olmesartan in healthy chinese volunteers. *Curr Ther Res Clin Exp* **76**:7-10.

Liu S, Beringer PM, Hidayat L, Rao AP, Louie S, Burckart GJ and Shapiro B (2008) Probenecid, but not cystic fibrosis, alters the total and renal clearance of fexofenadine. *J Clin Pharmacol* **48**:957-965.

Lombardo F, Obach RS, Varma MV, Stringer R and Berellini G (2014) Clearance Mechanism Assignment and Total Clearance Prediction in Human based upon In Silico Models. *J Med Chem* **57**:4397-4405.

Maeda K, Tian Y, Fujita T, Ikeda Y, Kumagai Y, Kondo T, Tanabe K, Nakayama H, Horita S, Kusuhara H and Sugiyama Y (2014) Inhibitory effects of p-aminohippurate and probenecid on the renal clearance of adefovir and benzylpenicillin as probe drugs for organic anion transporter (OAT) 1 and OAT3 in humans. *Eur J Pharm Sci* **59**:94-103.

Massarella JW, Nazareno LA, Passe S and Min B (1996) The effect of probenecid on the pharmacokinetics of zalcitabine in HIV-positive patients. *Pharm Res* **13**:449-452.

Mikkaichi T, Suzuki T, Onogawa T, Tanemoto M, Mizutamari H, Okada M, Chaki T, Masuda S, Tokui T, Eto N, Abe M, Satoh F, Unno M, Hishinuma T, Inui K, Ito S, Goto J and Abe T (2004) Isolation and characterization of a digoxin transporter and its rat homologue expressed in the kidney. *Proc Natl Acad Sci U S A* **101**:3569-3574.

Morrissey KM, Stocker SL, Wittwer MB, Xu L and Giacomini KM (2013) Renal transporters in drug development. *Ann Rev Pharmacol Toxicol* **53**:503-529.

Obach RS, Baxter JG, Liston TE, Silber BM, Jones BC, Macintyre F, Rance DJ and Wastall P (1997) The prediction of human pharmacokinetic parameters from preclinical and in vitro metabolism data. *J Pharmacol Exp Ther* **283**:46-58.

Obach RS, Lombardo F and Waters NJ (2008) Trend analysis of a database of intravenous pharmacokinetic parameters in humans for 670 drug compounds. *Drug Metab Dispos* **36**:1385-1405.

Odlind B, Beermann B and Lindstrom B (1983) Coupling between renal tubular secretion and effect of bumetanide. *Clin Pharmacol Ther* **34**:805-809.

Paine SW, Ménochet K, Denton R, McGinnity DF and Riley RJ (2011) Prediction of human renal clearance from preclinical species for a diverse set of drugs that exhibit both active secretion and net reabsorption. *Drug Metab Dispos* **39**:1008-1013.

Poirier A, Lavé T, Portmann R, Brun M-E, Senner F, Kansy M, Grimm H-P and Funk C (2008) Design, data analysis, and simulation of in vitro drug transport kinetic experiments using a mechanistic in vitro model. *Drug Metab Dispos* **36**:2434-2444.

Posada MM, Bacon JA, Schneck KB, Tirona RG, Kim RB, Higgins JW, Pak YA, Hall SD and Hillgren KM (2015) Prediction of renal transporter mediated drug-drug interactions for pemetrexed using physiologically based pharmacokinetic modeling. *Drug Metab Dispos* **43**:325-334.

Russel FG, Masereeuw R and van Aubel RA (2002) Molecular aspects of renal anionic drug transport. *Ann Rev Physiol* **64**:563-594.

Scotcher D, Jones C, Rostami-Hodjegan A and Galetin A (2016) Novel minimal physiologically-based model for the prediction of passive tubular reabsorption and renal excretion clearance. *Eur J Pharm Sci*.

Selen A, Amidon GL and Welling PG (1982) Pharmacokinetics of probenecid following oral doses to human volunteers. *J Pharm Sci* **71**:1238-1242.

Shen H, Liu T, Morse BL, Zhao Y, Zhang Y, Qiu X, Chen C, Lewin AC, Wang XT, Liu G, Christopher LJ, Marathe P and Lai Y (2015) Characterization of Organic Anion Transporter 2 (SLC22A7): A Highly Efficient Transporter for Creatinine and Species-Dependent Renal Tubular Expression. *Drug Metab Dispos* **43**:984-993.

Sirianni GL and Pang KS (1997) Organ clearance concepts: new perspectives on old principles. *J Pharmacokinet Biopharm* **25**:449-470.

USFDA (2012) Drug interaction studies - study design, data analysis, implications for dosing, and labeling recommendations. *http://wwwfdagov/downloads/drugs/guidancecomplianceregulatoryinformation/guidances/ucm292362pdf Center for Drug Evaluation and Research (CDER), Rockville, MD*.

Varma MV, Feng B, Obach RS, Troutman MD, Chupka J, Miller HR and El-Kattan A (2009) Physicochemical determinants of human renal clearance. *J Med Chem* **52**:4844-4852.

Varma MV, Gardner I, Steyn SJ, Nkansah P, Rotter CJ, Whitney-Pickett C, Zhang H, Di L, Cram M and Fenner KS (2012) pH-dependent solubility and permeability criteria for provisional biopharmaceutics classification (BCS and BDDCS) in early drug discovery. *Mol Pharm* **9**:1199-1212.

Varma MV, Steyn SJ, Allerton C and El-Kattan AF (2015) Predicting clearance mechanism in drug discovery: extended clearance classification system (ECCS). *Pharm Res* **32**:3785-3802.

Watanabe T, Kusuhara H, Watanabe T, Debori Y, Maeda K, Kondo T, Nakayama H, Horita S, Ogilvie BW, Parkinson A and Hu Z (2011) Prediction of the overall renal tubular secretion and hepatic clearance of anionic drugs and a renal drug-drug interaction involving organic anion transporter 3 in humans by in vitro uptake experiments. *Drug Metab Dispos* **39**:1031-1038.

Wu C-Y and Benet LZ (2005) Predicting drug disposition via application of BCS: transport/absorption/elimination interplay and development of a biopharmaceutics drug disposition classification system. *Pharm Res* **22**:11-23.

Yasui-Furukori N, Uno T, Sugawara K and Tateishi T (2005) Different effects of three transporting inhibitors, verapamil, cimetidine, and probenecid, on fexofenadine pharmacokinetics. *Clin Pharmacol Ther* **77**:17-23.

FOOTNOTES

All authors are full-time employees of Pfizer Inc. The authors have no conflicts of interest that are directly relevant to this study.

LEGENDS FOR FIGURES:

Fig. 1. Time-course of uptake by OATs-transfected and wild-type HEK293 cells of selective substrates. Curves represent data fitting to 2-compartment model to estimate active and passive intrinsic clearances.

Fig. 2. *In vitro–in vivo* extrapolation to predict intrinsic secretory clearance (A) and total plasma renal clearance (B) of 31 drugs. Red, blue and green data points represent OAT1, OAT2 and OAT3 selective substrates, respectively. Diagonal solid, dashed and dotted lines represent unity, 2-fold and 3-fold error, respectively.

Fig. 3. Predicted contribution of OAT1, OAT2, OAT3 and glomerular filtration to the renal clearance of drugs evaluated. Gemfibrozil was not shown as the predicted active secretion is negligible.

Fig. 4. Correlation between apparent permeability and tubular fraction reabsorbed. (A) Correlation was established using a separate dataset of non-bases (closed points, n=31) employing Hill model. Curve represent data fit (shaded area – 95% confidence interval) of non-bases to sigmoidal model, $F_{reabs} = P_{app}^{a}/(b^{a} + P_{app}^{a})$. Bases (open points, n=16) did not show distinct trend and were not considered for model fitting. Vertical dotted line represent ECCS permeability cut-off. (B) Predicted renal fraction reabsorbed of the compounds in the current OATs dataset on the basis of established correlation.

Fig. 5. Probenecid concentration-dependent inhibition of OAT1-mediated PAH uptake, OAT2-mediated cGMP uptake and OAT3-mediated E3S uptake in transfected cells. Mean (and 95% CI) of inhibition constant (IC_{50}) against each OAT is provided. Each data point represent mean±s.d. of n=3.

Fig. 6. Observed versus predicted change in human renal clearance of the OAT substrate drugs when coadministered with probenecid. Mechanistic static model predicted and observed values are within 40% for 16 of 18 (89%) cases. Diagonal solid and dashed lines represent unity and ±25% and ±40% error. Dotted horizontal and vertical lines represent bioequivalence limits.

Table. 1. Summary of *in vitro* mean intrinsic transport clearances obtained using HEK293 cells and predicted secretory and total renal clearance of 31 drugs investigated.

Compounds	ECCS class	HEK WT-Passive uptake CL_{pass} (µL/min/mg)	OAT1 Active uptake $CL_{int,OAT1}$ (µL/min/mg)	OAT2 Active uptake $CL_{int,OAT2}$ (µL/min/mg)	OAT3 Active uptake $CL_{int,OAT3}$ (µL/min/mg)	$f_{u,p}$	*Blood-to-plasma ratio*	Predicted $CL_{int,sec}$ (mL/min/kg)	Observed $CL_{int,sec}$ (mL/min/kg)	Predicted $CL_{renal,p}$ (mL/min/kg)	Observed $CL_{renal,p}$ (mL/min/kg)	Observed total plasma Clearance (mL/min/kg)
Acetazolamide	3A	3.0*	1.1	<2[†]	4.1*	0.04	0.55	1.1	15.4	0.12	0.65	0.65
Acyclovir (OAT2)[⊥]	4	0.3*	0.0	4.6*	0.1	0.85	1.00	2.2	2.7	3.18	3.50	4.70
Adefovir	3A	2.8*	146.0*	<2	3.5	0.96	0.55	7.0	2.1	5.47	3.33	3.70
Amoxicillin	3A	4.6	2.9	<2	4.3	0.850	0.55	1.2	1.0	2.46	2.26	3.30
Benzylpenicillin (OAT3)[⊥]	3A	4.8	0.0	<2	84.1*	0.4	0.66	22.2	22.5	5.49	5.53	7.00
Bumetanide	3A	0.3	4.7*	<2	27.9*	0.03	1.00	7.6	28.0	0.28	0.85	2.50
Captopril	3A	17.8*	3.8	<2	80.6*	0.73	1.20	21.4	33.9	9.84	12.00	12.00
Cefazolin	3B	1.7	1.3	<2	7.1*	0.31	0.55	1.9	0.8	1.11	0.80	0.89
Cefdinir	3A	1.0	0.0	<2	9.5*	0.4	1.00	2.5	4.5	1.65	2.34	2.41
Cefotaxime	3B	3.3	2.2	<2	6.4*	0.6	0.55	1.8	0.6	2.01	1.40	2.70
Cilostazol	4	11.0*	10.2*	<2	0.0	0.02	1.00	0.4	0.2	0.04	0.04	2.60
Cimetidine	4	14.4*	0.0	<2	63.9*	0.81	1.00	16.9	13.5	8.74	7.90	8.10
Famotidine	4	2.2*	0.8	<2	30.8*	0.83	0.55	8.2	5.4	5.27	4.42	6.60
Fexofenadine	3B	0.0*	19.4*	<2	8.8*	0.31	0.70	3.1	3.2	1.44	1.47	11.00
Furosemide	3A	36.4	0.0	<2	570.0*	0.012	1.00	150.1	156.6	1.64	1.70	2.40
Ganciclovir (OAT2)[⊥]	4	0.1	0.0	9.0*	0.1	0.985	0.55	4.3	3.3	4.59	4.10	4.60
Gemfibrozil	1A	31.0*	3.0	<2	0.3	0.008	1.00	0.2	0.3	0.02	0.02	1.70
Gemfibrozil Glucuronide	3B	0.1	13.2	<2	5.8	0.115	0.83	2.1	2.9	0.44	0.53	1.24
Hydrochlorothiazide	4	0.1	47.0*	<2	33.0*	0.42	0.60	10.6	15.9	3.78	4.66	4.90
Ketoprofen	1A	91.0*	209.0*	<2	0.0	0.008	0.55	8.6	8.3	0.08	0.08	1.60
Ketorolac	1A	22.7*	424.0*	15.3*	0.0	0.0068	1.00	24.7	27.4	0.18	0.20	0.35
Methotrexate	3B	2.0	4.0	<2	24.8	0.37	0.83	6.7	3.1	2.74	1.70	2.10
Olmesartan	3B	12.0	45.0	<2	56.0	0.01	0.55	16.6	12.7	0.18	0.14	0.31
Oseltamivir acid (OAT3)[⊥]	3A	0.0	0.0	<2	14.6*	0.97	0.83	3.9	3.6	4.63	4.50	4.80
Penciclovir	4	0.5*	0.1	13.5*	1.0*	0.85	0.55	6.6	15.2	4.93	6.69	9.36
Pravastatin	3B	0.2	0.2	<2	13.8*	0.55	0.56	3.6	25.1	2.61	6.35	13.50
Rosuvastatin	3B	0.0	0.0	<2	28.2*	0.12	0.69	7.4	36.0	1.04	3.30	11.00
Sitagliptin	4	6.3	0.1	<2	49.7*	0.61	1.12	13.1	7.6	6.58	4.74	6.00
Tenofovir (OAT1)[⊥]	3A	0.1	30.9*	<2	0.3	0.92	0.55	1.4	1.3	2.72	2.70	3.10
Torsemide	3A	4.5*	22.0*	<2	29.0*	0.01	0.55	8.6	11.4	0.10	0.13	0.53
Zalcitabine	4	7.1	0.0	<2	57.6*	0.96	1.00	15.2	2.8	9.27	3.97	5.60

[⊥]Selective substrates of OATs.

[†]Implies uptake ratio of <2 (uptake by OAT2 to wild-type ratio) at 3 min. Rates in OAT2 cells were measured only for compounds showing uptake ratio >2, in an initial study.

*Simultaneous dynamic model fit of wild-type and OATs transport data yielded values for the lower limit of 95% confidence interval above zero. For others estimated rates are not statistically discernable from zero.

Table 2. Summary of mechanistic static model based predictions of OAT-mediated DDIs with probenecid

Compounds	Probenecid dose	Predicted Change in CL_{Sec} (%)	Predicted change in renal clearance (%)	Observed change in renal clearance (%)	Predicted/Observed ratio	References for observed change in renal clearance
Acyclovir	1g	3	2	32	0.05	(Laskin et al., 1982)
Adefovir	0.5g	29	20	15	1.32	(Maeda et al., 2014)
Adefovir	0.75g	50	34	56	0.61	(Maeda et al., 2014)
Adefovir	1.5g	76	53	48	1.09	(Maeda et al., 2014)
Benzylpenicillin	0.5g	43	37	50	0.74	(Maeda et al., 2014)
Benzylpenicillin	0.75g	65	56	54	1.04	(Maeda et al., 2014)
Benzylpenicillin	1.5g	86	75	78	0.96	(Maeda et al., 2014)
Bumetanide	1g	84	68	85	0.80	(Odlind et al., 1983)
Cefazolin	1g	83	42	38[⊥]	1.10	(Brown et al., 1993)
Cimetidine	0.5g	42	35	25	1.42	(Gisclon et al., 1989)
famotidine	1.5g	86	62	64	0.97	(Inotsume et al., 1990)
Fexofenadine	1g	80	49	68	0.72	(Yasuhara-Furukori et al., 2005; Liu et al., 2008)
Furosemide	1g	83	82	72	1.14	(Chennavasin et al., 1979)
Ganciclovir	1g	2	1	19	0.08	(Cimoch et al., 1998)
Methotrexate	1g	82	62	55	1.13	(Aherne et al., 1978)
Olmesartan	0.5g	55	50	33	1.51	(Li et al., 2014)
Oseltamivir acid	0.5g	52	32	52[⊥]	0.62	(Hill et al., 2002)
Zalcitabine	0.5g	42	34	42	0.81	(Massarella et al., 1996)

[⊥]Change in renal clearance was assumed to be same as change in total IV clearance.

Predictions were based on mean transport rates from Table 1.

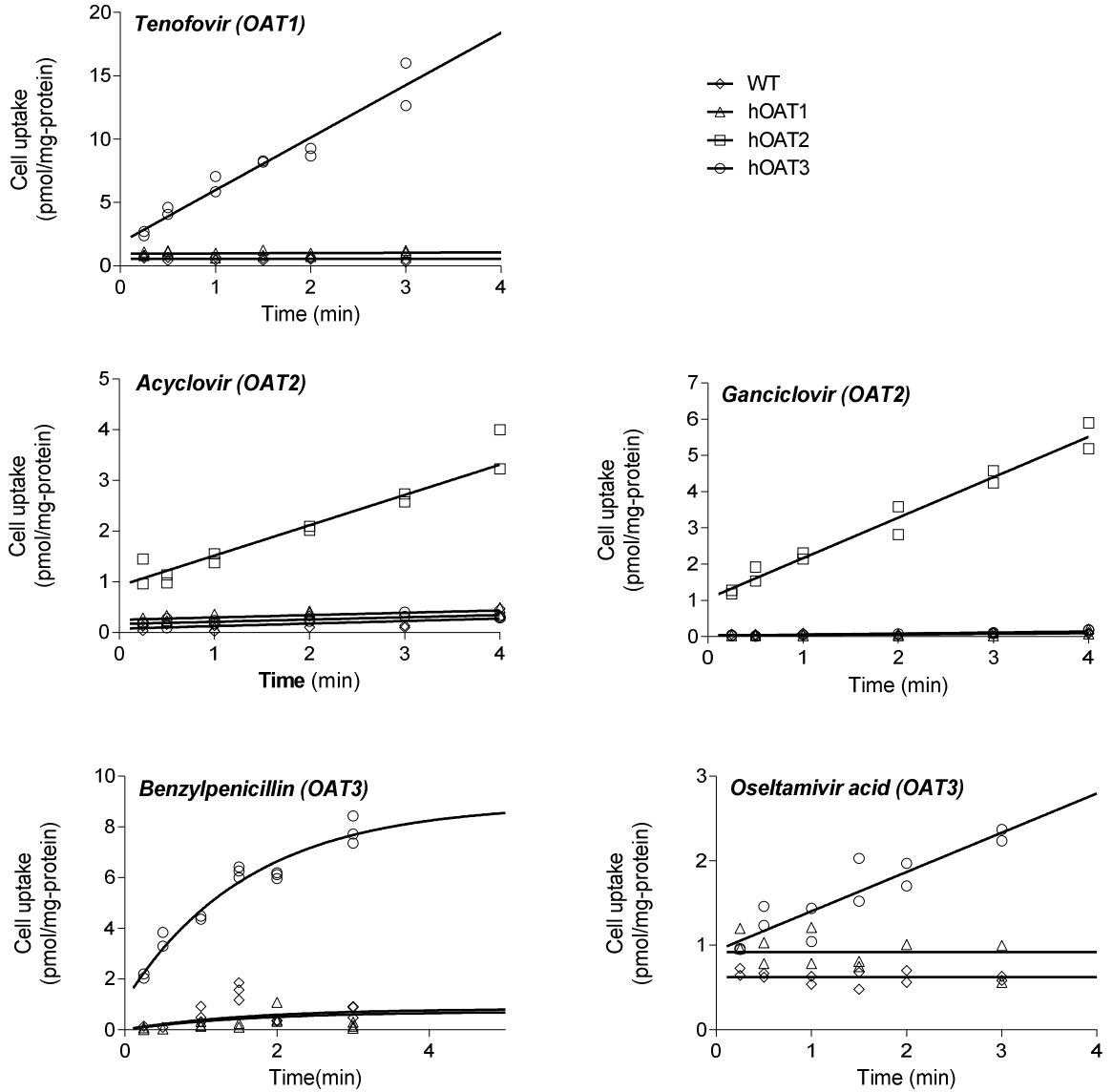
Tenofovir (OAT1)
Cell uptake (pmol/mg-protein)
Time (min)
WT
hOAT1
hOAT2
hOAT3
Acyclovir (OAT2)
Cell uptake (pmol/mg-protein)
Time (min)
Ganciclovir (OAT2)
Cell uptake (pmol/mg-protein)
Time (min)
Benzylpenicillin (OAT3)
Cell uptake (pmol/mg-protein)
Time(min)
Oseltamivir acid (OAT3)
Cell uptake (pmol/mg-protein)
Time (min)

Fig. 1.

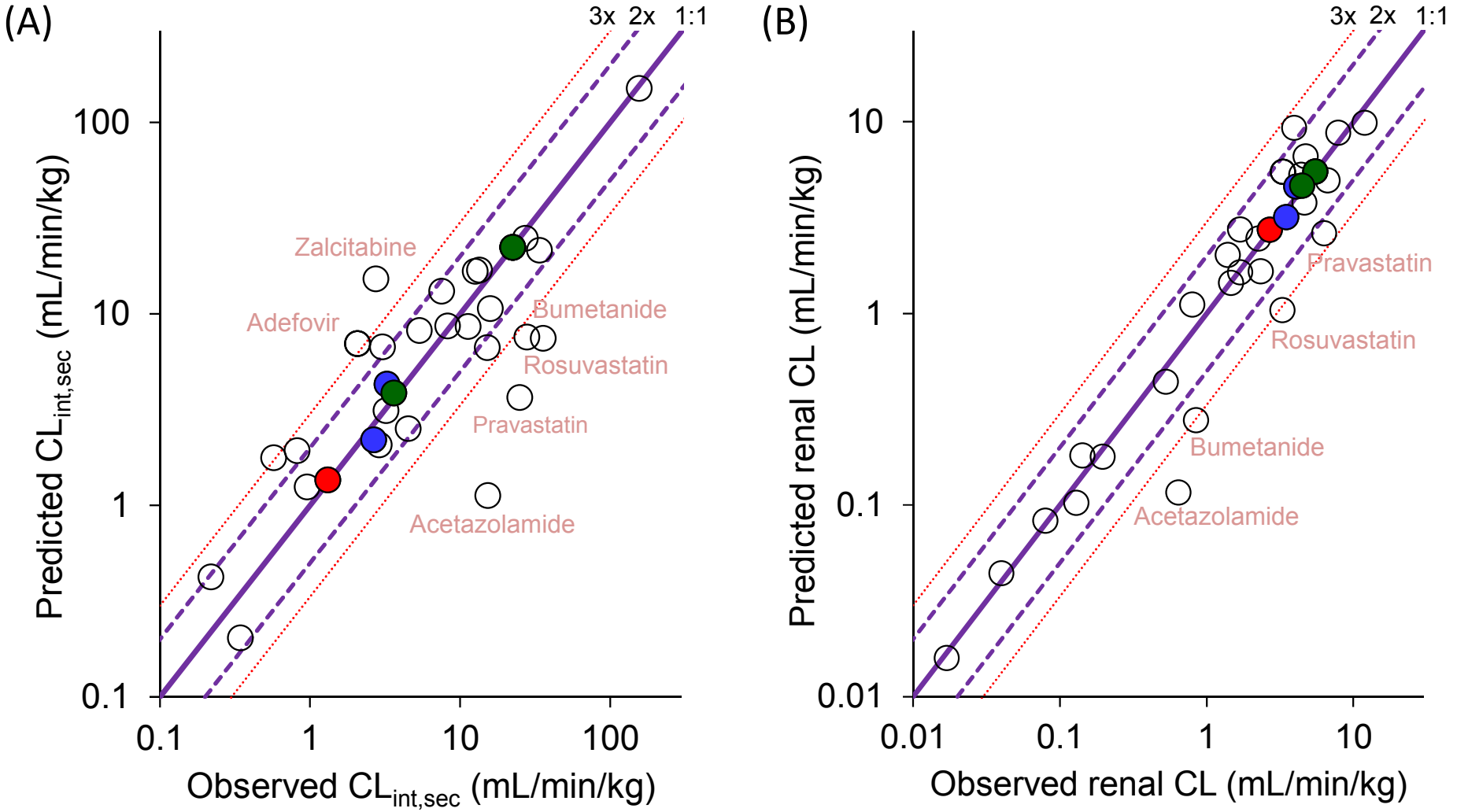
(A)
3x 2x 1:1
Predicted $CL_{int,sec}$ (mL/min/kg)
Observed $CL_{int,sec}$ (mL/min/kg)
100
10
1
0.1
0.1
1
10
100
Zalcitabine
Adefovir
Bumetanide
Rosuvastatin
Pravastatin
Acetazolamide
(B)
3x 2x 1:1
Predicted renal CL (mL/min/kg)
Observed renal CL (mL/min/kg)
10
1
0.1
0.01
0.01
0.1
1
10
Pravastatin
Rosuvastatin
Bumetanide
Acetazolamide

Fig. 2.

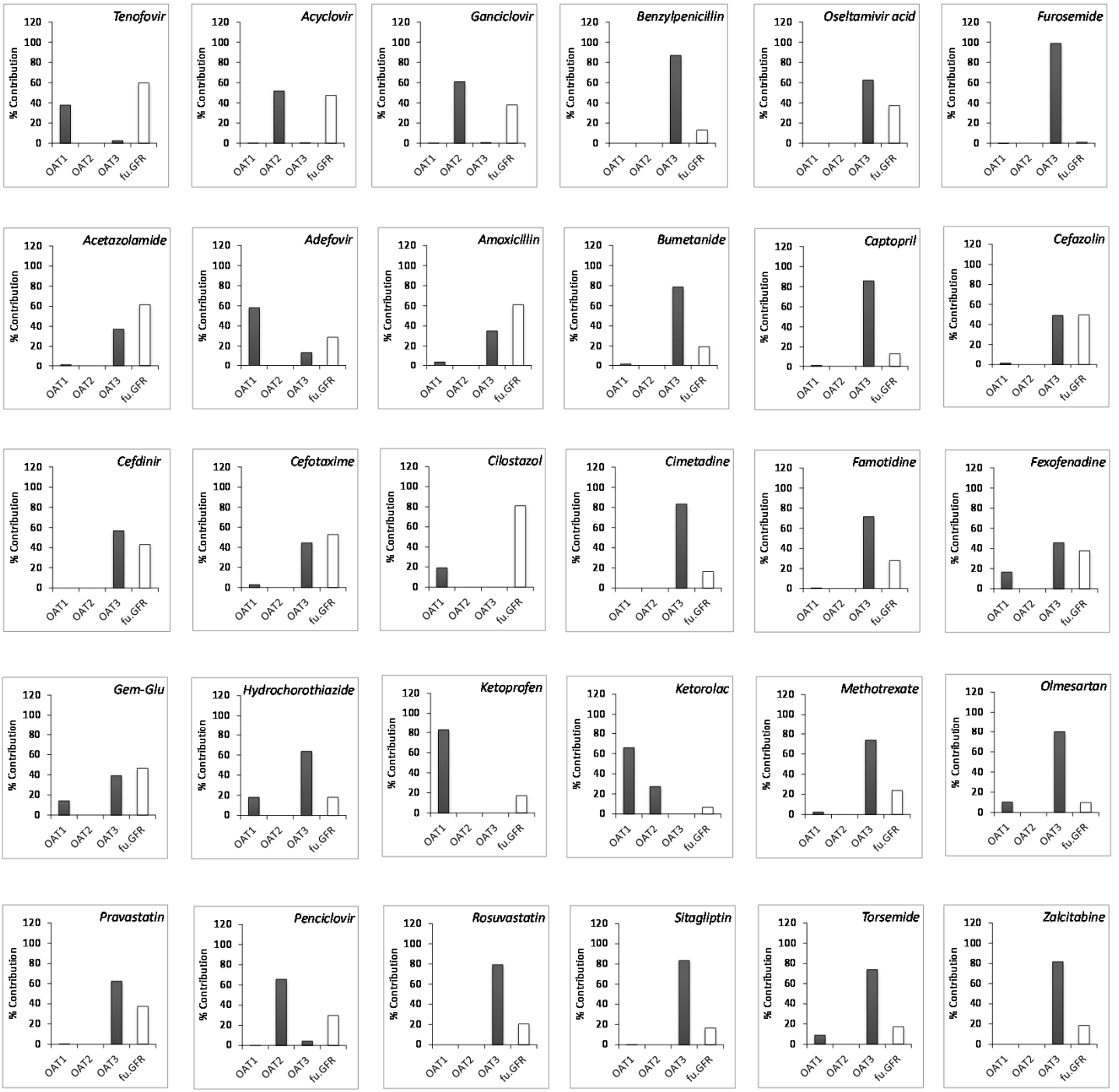

Fig. 3.

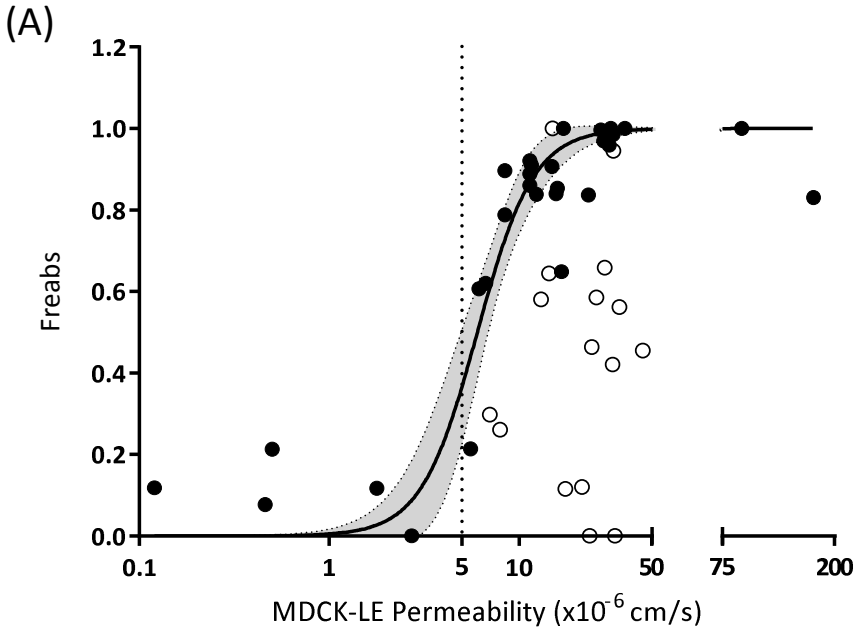
(A)
1.2
1.0
0.8
0.6
0.4
0.2
0.0
Freabs
0.1
1
5
10
50
75
200
MDCK-LE Permeability (x10-6 cm/s)

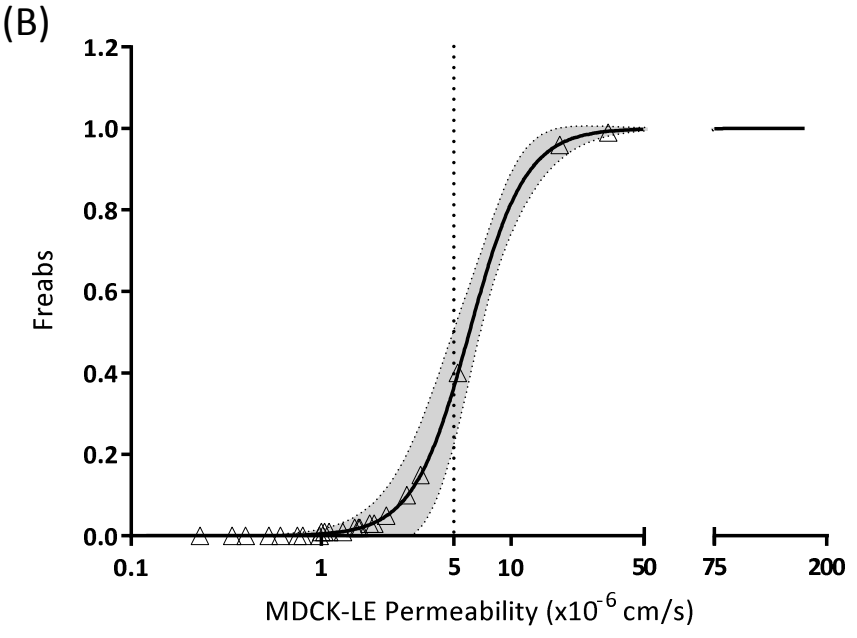
(B)
1.2
1.0
0.8
0.6
0.4
0.2
0.0
Freabs
0.1
1
5
10
50
75
200
MDCK-LE Permeability (x10-6 cm/s)

Fig. 4.

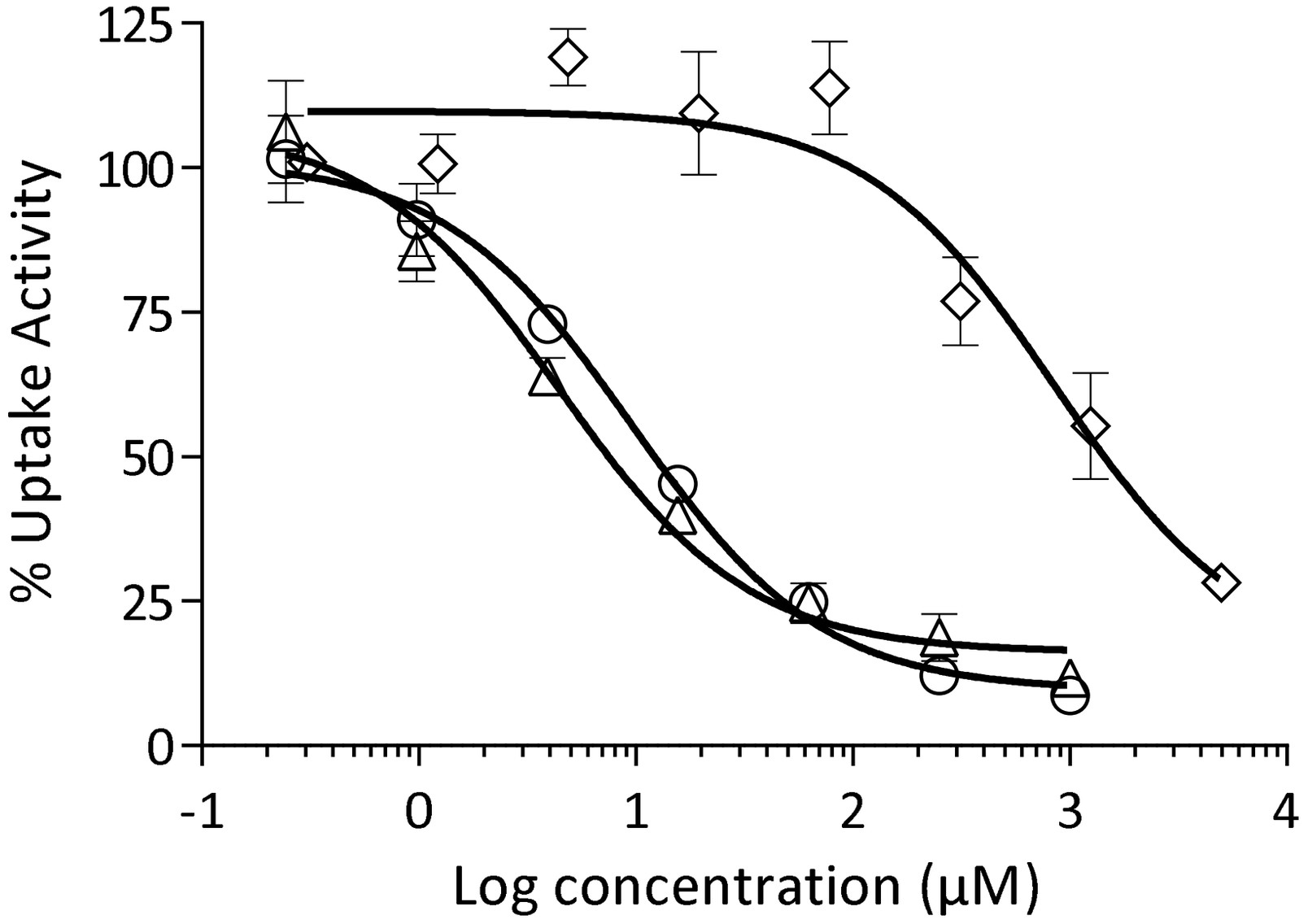
125
100
75
50
25
0
% Uptake Activity
-1
0
1
2
3
4
Log concentration (µM)
OAT1 IC50 (µM) = 9.6 (7.5-12.3)
OAT2 IC50 (µM) = 853 (409-1779)
OAT3 IC50 (µM) = 4.5 (3.1-6.4)

Fig. 5.

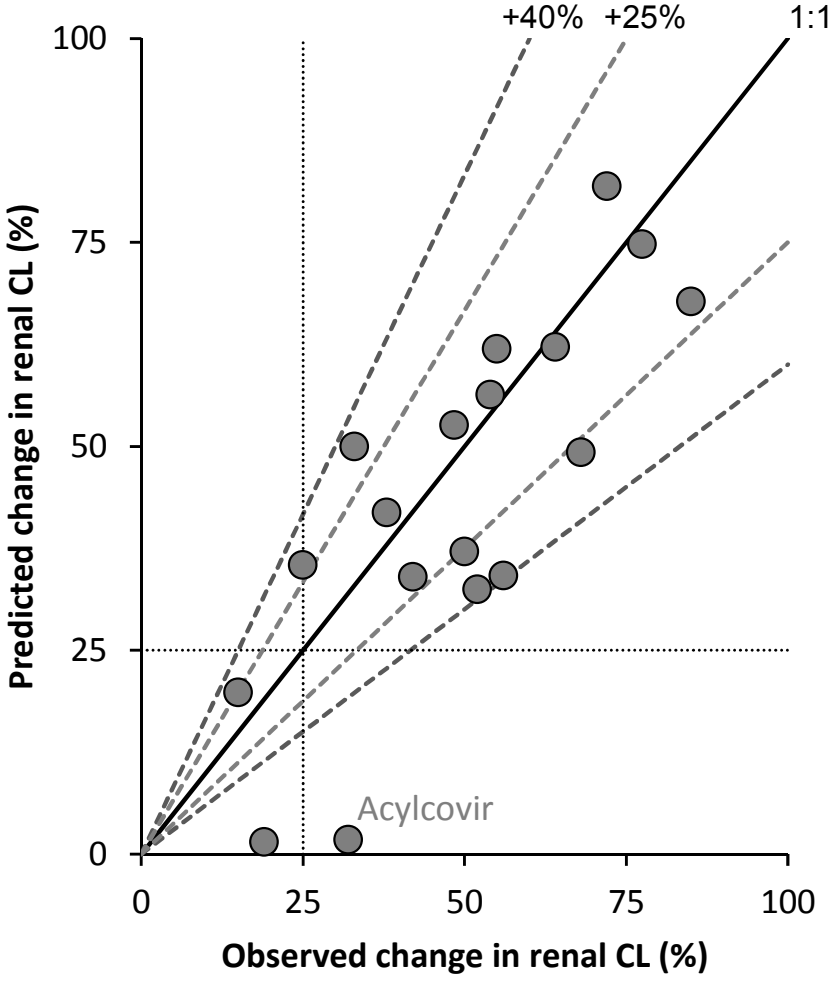
+40%
+25%
1:1
100
75
50
25
0
Predicted change in renal CL (%)
Acylcovir
0
25
50
75
100
Observed change in renal CL (%)

Fig. 6.

Quantitative prediction of human renal clearance and drug-drug interactions of organic anion transporter substrates using *in vitro* transport data: A relative activity factor approach

Sumathy Mathialagan, Mary Piotrowski, David A Tess, Bo Feng, John Litchfield, Manthena V Varma

Pharmacokinetics, Pharmacodynamics, and Metabolism Department – New Chemical Entities, Pfizer Inc., Eastern Point Road, Groton, CT (SM., MP., BF., MV.) and Cambridge MA (DT., JL.)

Journal: ***Drug Metabolism Disposition***

Supplementary Table 1. Dataset of compounds used to establish permeability-fraction reabsorbed relationship. Apparent permeability across MDCK-low efflux cellines was measured at apical pH 6.5 and basolateral pH 7.4. (Varma et al. 2009). Human renal clearance and fraction reabsorbed (F_{reabs}) were extracted from Varma et al. 2009. For comparison, recently compiled F_{reabs} (Scotcher et al. 2016) were also presented.

Ionic state	Compound	MDCK-LE Papp (10^{-6} cm/s) pH 6.5	*Human renal CL (mL/min/kg)*	*fu*GFR*	F_{reabs} (Varma et al 2009)	F_{reabs} (Scotcher et al. 2016)
A	Chlorpropamide	11.60	0.008	0.089	0.91	0.91
A	Glipizide	5.55	0.03	0.04	0.21	
A	Glyburide	17.09	0.00	0.04	1.00	
A	Irbesartan	6.66	0.03	0.089	0.62	0.62
A	Isoxicam	26.95	0.00	0.0712	1.00	1.00
A	Sulfamethoxazole	8.40	0.06	0.623	0.90	0.89
A	Warfarin	29.75	0.00	0.03	0.96	
B	Betaxolol	17.50	0.71	0.80	0.12	0.08
B	Chlorpheniramine	28.21	0.43	1.25	0.66	0.26
B	Desipramine	7.00	0.20	0.28	0.30	
B	Diphenhydramine	31.00	0.20	0.34	0.42	
B	Doxepin	14.33	0.14	0.3916	0.64	0.64
B	Imipramine	13.06	0.10	0.2314	0.58	0.55
B	Itraconazole	15.00	0.00	0.00	1.00	
B	Lidocaine	44.71	0.32	0.59	0.46	
B	Metoclopromide	23.49	1.14	1.07	0.00	
B	Metoprolol	25.54	0.65	1.57	0.59	-0.05
B	Mexiletine	31.90	1.02	0.8544	0.00	-0.25
B	Moclobemide	31.40	0.05	0.89	0.95	0.94
B	Oxprenolol	24.11	0.13	0.2492	0.46	0.44
B	Propafenone	7.92	0.11	0.1424	0.26	0.26
B	Ropivacaine	33.66	0.04	0.089	0.56	0.55
B	Venlafaxine	21.40	1.14	1.2994	0.12	0.09
N	Acetaminophen	12.32	0.15	0.93	0.84	
N	Antipyrine	31.13	0.02	1.66	0.99	0.99
N	Betamethasone	8.40	0.14	0.64	0.79	0.78
N	Caffeine	31.18	0.02	1.14	0.99	0.99
N	Dapsone	23.14	0.08	0.4806	0.84	0.83
N	Diazepam	36.00	0.00	0.04	1.00	
N	Fluconazole	15.92	0.22	1.5308	0.85	0.86
N	Levetiracetam	16.70	0.56	1.602	0.65	0.64
N	Metronidazole	11.41	0.19	1.71	0.89	0.92
N	Midazolam	27.00	0.00	0.03	1.00	
N	Nifedipine	88.93	0.00	0.08	1.00	
N	Prednisone	14.88	0.05	0.48	0.91	0.30
N	Propylthiouracil	15.60	0.05	0.2848	0.84	0.83
N	Ribavirin	0.12	1.57	1.78	0.12	0.08
N	Tacrolimus	6.14	0.01	0.02	0.61	
N	Theophylline	11.40	0.09	1.09	0.92	0.91
N	Topiramate	11.40	0.22	1.5486	0.86	0.86
N	Voriconazole	27.91	0.02	0.7476	0.97	0.97
Z	Doxycycline	1.78	0.19	0.21	0.12	
Z	Gabapentin	0.50	1.36	1.7266	0.21	0.18
Z	Levodopa	166.08	0.23	1.35	0.83	
Z	Levofloxacin	2.71	1.41	1.34	0.00	
Z	Lisinopril	0.46	1.20	1.30	0.08	
Z	Rosiglitazone	30.34	0.00	0.00	1.00	

Supplementary Table 2. Summary of the literature knowledge on the substrate affinity to renal uptake and efflux transporters based on *in vitro* transport studies of 31 drugs investigated. Source of the transporter activity is University of Washington drug interaction database (https://www.druginteractioninfo.org).

Compounds	Basolateral uptake transporters	Apical efflux transporters
Acetazolamide		
Acyclovir	OAT1, OAT2, OAT3	MATE1, MATE2-K
Adefovir	OAT1, OAT3	P-gp, MRP4
Amoxicillin	OAT1	
Benzylpenicillin	OAT1, OAT3	
Bumetanide	OAT1, OAT2, OAT3	OAT4
Captopril	OAT1, OAT3	
Cefazolin	OAT3	MRP4
Cefdinir	OAT1, OAT3	MRP4
Cefotaxime	OAT2, OAT3	OAT4, MRP4
Cilostazol	OAT3	
Cimetidine	OAT1, OAT2, OAT3, OCT2	P-gp, MATE1, MATE2-K
Famotidine	OAT3, OCT2	P-gp
Fexofenadine	OAT3	P-gp
Furosemide	OAT1, OAT3	MRP2
Ganciclovir	OAT1, OAT2	MATE1, MATE2-K
Gemfibrozil		
Gemfibrozil Glucuronide		MRP2
Hydrochlorothiazide	OAT1, OAT3	P-gp
Ketoprofen	OAT1, OAT3	OAT4
Ketorolac		
Methotrexate	OAT1, OAT2, OAT3	OAT4, MRP2, MRP4
Olmesartan	OAT1, OAT3	OAT4, MRP2, MRP4
Oseltamivir acid	OAT1, OAT3	MRP4
Penciclovir	OAT2	
Pravastatin	OAT3	OAT4, MRP2
Rosuvastatin	OAT3	MRP4
Sitagliptin	OAT3, OATP4C1	P-gp
Tenofovir	OAT1, OAT3, OATP4C1	P-gp, MRP4
Torsemide		
Zalcitabine		